DOI: 10.18721/JPM.14202
UDC 546.03.535.015

PHASE TRANSITIONS AND DIFFUSE REFLECTANCE SPECTRA OF BARIUM TITANATE-ZIRCONATE SOLID SOLUTIONS

M.M. Mikhailov[1], **O.A. Alekseeva**[1], **S.A. Yuryev**[1], **A.N. Lapin**[1], **E.Yu. Koroleva**[2]

[1] Tomsk State University of Control Systems and Radioelectronics, Tomsk, Russian Federation;

[2] Peter the Great St. Petersburg Polytechnic University, St. Petersburg, Russian Federation

The composition, structure, particle size distribution, diffuse reflectance spectra, integral absorption coefficients of solar radiation and dielectric properties of $BaTi(1-x)Zr(x)O_3$ powders synthesized from micro powders $BaCO_3$, ZrO_2 and TiO_2 at $x = 0 - 0.3$ have been studied. Changes in the integral absorption coefficient of the powders at different concentrations of zirconium cations were found to be within 34 %. Dielectric studies conducted over the wide ranges of temperature and frequency showed the presence of two phase transitions, one of them undergoing near the room temperatures. This fact makes it possible to consider these powders as pigments for thermal control coatings at operating temperatures of space crafts.

Keywords: barium titanate-zirconate, thermal control coating, phase transition, diffuse reflectance spectrum

Citation: Mikhailov M.M., Alekseeva O.A., Yuryev S.A., Lapin A.N., Koroleva E.Yu., Phase transitions and diffuse reflectance spectra of barium titanate-zirconate solid solutions, St. Petersburg Polytechnical State University Journal. Physics and Mathematics. 14 (2) (2021) 16–27. DOI: 10.18721/JPM.14202

ФАЗОВЫЕ ПЕРЕХОДЫ И СПЕКТРЫ ДИФФУЗНОГО ОТРАЖЕНИЯ ТВЕРДЫХ РАСТВОРОВ ТИТАНАТА-ЦИРКОНАТА БАРИЯ

М.М. Михайлов[1], **О.А. Алексеева**[1], **С.А. Юрьев**[1], **А.Н. Лапин**[1], **Е.Ю. Королева**[2]

[1] Томский государственный университет систем управления и радиоэлектроники, г. Томск, Российская Федерация;

[2] Санкт-Петербургский политехнический университет Петра Великого, Санкт-Петербург, Российская Федерация

Исследованы состав, структура, гранулометрический состав, спектры диффузного отражения, интегральные коэффициенты поглощения солнечного излучения и диэлектрические свойства порошков $BaTi(1-x)Zr(x)O_3$, синтезированных из микропорошков $BaCO_3$, ZrO_2 и TiO_2 при концентрации замещающих катионов циркония в диапазоне значений x от 0 до 0,3. Установлены изменения интегрального коэффициента поглощения исследованных порошков при различной концентрации замещающих катионов циркония в пределах 34 %. Диэлектрические исследования, проведенные в широком температурном и частотном диапазонах, выявили существование двух фазовых переходов в исследованных соединениях. Определены температуры фазовых переходов; установлено, что низкотемпературный фазовый переход происходит при комнатных температурах, что позволяет рассматривать данные

порошки в качестве пигментов для термостабилизирующих покрытий космических аппаратов при рабочих температурах.

Ключевые слова: титанат-цирконат бария, термостабилизирующее покрытие, фазовый переход, спектр диффузного отражения

Ссылка при цитировании: Михайлов М.М., Алексеева О.А., Юрьев С.А., Лапин А.Н., Королева Е.Ю. Фазовые переходы и спектры диффузного отражения твердых растворов титаната-цирконата бария // Научно-технические ведомости СПбГПУ. Физико-математические науки. 2021. Т. 14. № 2. С. 16–27. DOI: 10.18721/JPM.14202

Introduction

There is now currently a growing interest to the studies of thermal control coatings, which can be used to maintain the temperature of the objects they are applied to stable [1, 2]. So-called intelligent coatings draw the most attention, since they are capable of modifying their functional physical properties in response to small environment changes. Such coatings are very promising in terms of thermal control applications, in particular space craft device, where their ability to change emittance and radiated power in response to the change in the environment or the absorbed energy allows stabilizing the temperature of the space craft working points.

Solid solutions with phase transitions (PT) accompanied by rearrangement of the crystalline structure can be used as pigments for thermal control coatings (TCC) of reflecting type; the PT are located in the range of operating temperatures of the unit. Solid solutions of barium titanate $BaTiO_3$ are solid solutions of this type with its barium or titanium cations partially substituted by cations of other elements. The Curie temperature for barium titanate $BaTiO_3$ is 120°C. Barium titanate has cubic structure above this temperature. As temperature T decreases, there is a structural transition into phases with tetragonal ($5 \le T \le 120$°C), rhombic ($-90 \le T \le +5$ °C) and rhombohedric ($T < -90$ °C) lattices. The electric [3], dielectric [4] and optical [5] properties change as well. The most significant modification of the indicated properties is observed in the neighborhood of the Curie point (in the transition from the cubic to the tetragonal syngony): there is a variance by several times in dielectric permittivity ε and by five orders of magnitude in electrical conductivity σ [3]. Optical properties can change as well [6].

The change of electrical properties in the domain of phase transitions leads to significant changes [6] of the barium titanate emittance, which depends on the carrier density, in a temperature range from the values characteristic of quasi-metallic state (0.10) to the value specific to dielectrics (0.96). In case the coating is heating up to the PT temperature, its emissivity increases dramatically, which results in thermal radiation rising and the coating temperature decreasing. In the opposite situation, i.e. when the coating temperature is below the operating one, there is an abrupt drop in emittance. This leads to a reduction of thermal radiation and, respectively, to the temperature rising back to the previous level. This is the basis of thermal stabilization in the operation area of the object with the thermal control coating on its surface.

For practical purposes, there is a need for coatings, which can operate at lower temperatures than that barium titanate can provide. A partial substitution of barium or titanium cations with other positive ions A or B forming solid solutions of $Ba_{1-x}A_xTiO_3$ or $BaTi_{1-x}B_xO_3$ type allows the Curie temperature to shift into lower value ranges [7]. The value of the shift and PT characteristics are defined by the type of the substituting element and its concentration. If we vary the type and concentration of the substituting elements A or B, as well as the conditions of the pigment production, we can control the phase transitions of the coatings produced on the basis of such compounds [8–10].

The objectives of this study included a solid-phase synthesis of the $BaTi_{1-x}Zr_xO_3$ com-

pound at various values of x, as well as finding its phase and particle-size distribution, phase transition temperature and other essential physical properties characterizing its ability to reflect solar radiation (there is a need for materials promising in terms of producing reflective coatings for space crafts).

In favor of the set goal, we subjected the synthesized samples to X-ray phase and particle-size distribution analysis, studied their dielectric properties, obtained and analyzed their diffuse reflectance spectra and integral absorption coefficients.

Samples and test procedure

This paper presents a solid-phase synthesis of solid $BaTi_{1-x}Zr_xO_3$ solution based on $BaCO_3$, ZrO_2 and TiO_2 micro powders at concentration of substituting zirconium cations in the range of 0–0.3.

The samples were produced by means of solid-phase synthesis from manufactured micro-sized $BaCO_3$, ZrO_2 and TiO_2 powders. For each concentration of substituting zirconium cations, we prepared a mixture of the initial $BaCO_3$, ZrO_2 and TiO_2 powders in such a way as to meet the set barium atoms/$Ti_{1-x}Zr_x$ compound ratio of 1:1 for the obtained $BaTi_{1-x}Zr_xO_3$ compound at each value of x in compliance with the molecular masses of the initial $BaCO_3$, ZrO_2 and TiO_2 powders. The barium carbonate micropowder was dissolved in distilled water agitated by ultrasonic waves; then we added the silicon dioxide and titanium dioxide micropowders to the solution. The obtained compound was mixed in a magnetic stirrer for 1 h. The mixture was dried at 150°C, ground in an agate mortar and subject to double heating under atmosphere: first it was heated at 800°C for 2 h, then (after completely cooled down) it was heated at 1200°C for 2 h. The rate of temperature elevation on average amounted to 50°C/min, of cooling – 9°C/min.

We studied the samples of $BaTi_{1-x}Zr_xO_3$ with six different concentration of substituting cations in the range from 0 to 30%: x = 0.01; 0.03; 0.10; 0.15; 0.20; 0.30. We studied particle-size distribution of $BaTi_{1-x}Zr_xO_3$ powders using Shimadzu SALD-2300 laser diffraction particle size analyzer. We employed Shimadzu XRD 6000 X-ray diffractometer to perform X-ray phase analysis (XRD).

For dielectric measurements, we pressed the powders under 10 MPa pressure into tablets 1 cm wide and 1 mm thick. We used gold contacts with a chromium sublayer as electrodes for better adhesion. In the course of the measurement, the samples were heated at 120°C for 30 min first to remove the adsorbed water.

We measured dielectric properties using a broad-band spectrometer Novocontrol BDS80 in the frequency range from 0.1 Hz to 10 MHz, with the scanning field amplitude of 10 V/cm; relative measurement error of impedance and capacity is approximately $3 \cdot 10^{-5}$. The measurements were performed in a heating/cooling mode, the temperature change rate amounted to 1–2°C/min, measurement temperatures ranged from –50 to 150°C.

To measure diffuse reflectance spectra, the $BaTi_{1-x}Zr_xO_3$ samples were pressed into supports 24 mm wide and 2 mm tall under the pressure of 1 MPa with hold time of 2 mm. For diffuse reflectance spectra, we used Shimadzu UV-3600 Plus spectrophotometer with an integrating sphere attachment (ISR-603) in a wavelength range from 200 to 2200 nm and resolution of 5 nm.

Test results and their discussion

X-ray phase analysis data. A diffraction spectra analysis of the synthesized barium titanate powders with partially substituted cations showed that the peaks of intensity correspond to $BaTiO_3$ or $BaTi_{1-x}Zr_xO_3$ compounds. As an example, Fig. 1 demonstrates an X-ray diagram of $BaZr_{0.1}Ti_{0.9}O_3$ powder (x = 0.1). Aside from the basic compound, the synthesized powders contained phases of $ZrTiO_4$ and $BaZrO_3$, as well as residual unreacted initial powders used in the synthesis: $BaCO_3$, ZrO_2 and TiO_2. A study of the obtained X-ray diagrams allowed us to conclude that the basic phase of the produced powders had a tetragonal structure.

Based on the obtained diffraction data, we calculated the content of various compounds in the synthesized $BaTi_{1-x}Zr_xO_3$ powders (Table 1). The yield of the main phase for all obtained sam-

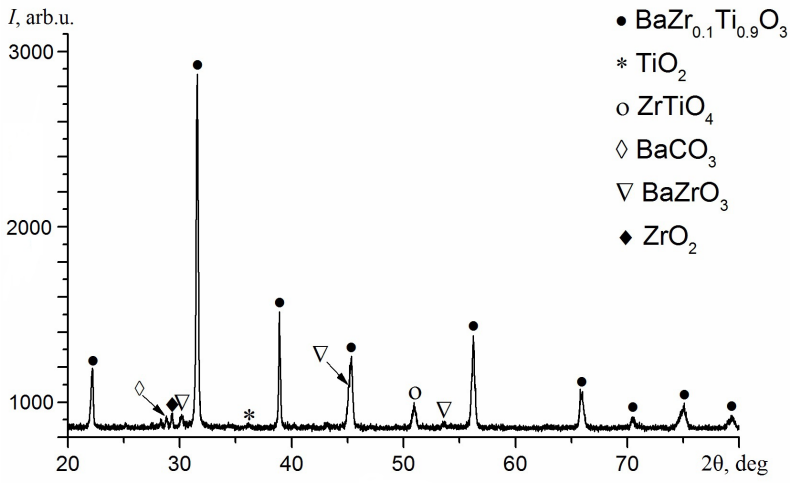

Fig. 1. X-ray diagram of $BaZr_{0.1}Ti_{0.9}O_3$ powder

Table 1

Percentage of different compounds in the synthesized $BaTi_{1-x}Zr_xO_3$ powders at $x = 0.01 - 0.30$

x	Compound composition, %					
	$BaTi_{1-x}Zr_xO_3/BaTiO_3$	ZrO_2	TiO_2	$ZrTiO_4$	$BaCO_3$	$BaZrO_3$
0.01	84.9	0.2	6.7	3.7	3.6	0.9
0.03	85.1	0.8	7.0	3.3	3.4	0.4
0.05	90.3	1.3	2.8	2.2	1.9	1.5
0.10	80.6	3.9	6.2	3.0	3.1	3.3
0.15	78.9	5.0	5.1	2.5	2.3	6.2
0.20	67.6	11.4	6.2	2.0	2.0	10.8
0.30	62.0	10.8	7.2	2.6	2.4	15.0

N o t e. The presented results were obtained on the basis of the X-ray phase analysis data.

ples containing from 0 to 0.3 of the substituting zirconium cations is in the range between 62.0 and 90.3%. The highest yield of the main phase (90.3%) is observed at the substituting zirconium cations concentration $x = 0.05$, while the lowest one (62%) – at $x = 0.30$. The content of $BaZrO_3$ and ZrO_2 phases grows with the increase in the substituting cations density. The percentage of the remaining non-essential phases in the synthesized solid solutions depends on the concentration of the substituting cations insignificantly and at various concentrations of $x = 0.01–0.30$ vary as follows:

TiO_2 – from 2.8 to 7.2 %,

$ZrTiO_4$ – from 2 to 3.7 %,

$BaCO_3$ – from 1.9 to 3.6 %.

Particle-size analysis data. The particle-size research showed that the synthesized powders contain particle of the size from 0.2 to 12 μm. The function of particles distribution for the $BaTi_{1-x}Zr_xO_3$ powders has a form of a curve with two peaks corresponding to the particle sizes of 0.51–0.53 μm and 2.30–2.67 μm respectively. With the change of the zirconium cations percentage from 1 to 30%, there is no significant shift of the distribution peaks (within the range of 0.02 and 0.37 μm for the first and the second peaks respectively), just as there is no considerable change in the intensity of the said peaks (up to 20% for the first peak and up to 10% for

the second one). The median particle size in the $BaTi_{1-x}Zr_xO_3$ powders ranges from 1.911 to 2.990 μm. The maximum median particle size is observed in the $BaTiO_3$ powder (2.196 μm) at the zirconium cation concentration equal to 0.15 (2.199 μm). The minimum median particle size (1.911 μm) corresponds to the maximum zirconium cation concentration equal to 0.03. The modal particle diameter (diameter with the highest incidence rate of grain sizes or a prevailing fraction) for all the powders under study was identical and equal to 2.234 μm.

Dielectric properties study. We can see two peaks on the permittivity temperature dependences of all the samples: a more prominent one is observed at the temperature range of 109–117°C and a less prominent one – at 27–47°C (Fig. 2). Note that the temperature values corresponding to the maximum permittivity during heating are lower than that during cooling down (see Fig. 2 for an example); for a high temperature peak in the range of 109–117°C the thermal lag is around 5°C. The respective data for the remaining values of x are similar.

In the entire temperature test range, we obtained and analyzed the frequency dependences of the real and imaginary components of permittivity ε'(ω), ε"(ω) for the solid $BaTi_{1-x}Zr_xO_3$ solutions. To describe the relaxation contributions, we used the Cole–Cole distribution, which allows describing the spectra extending over a wider range than Debye relaxation. As a model function, we applied a sum of DC conductivity, several relaxation processes and high-frequency conductivity contributions:

$$\varepsilon^*(\omega) = \varepsilon_\infty + \sum_{i=1}^{n} CC_i + j\frac{\sigma_{DC}}{\omega\varepsilon_0} =$$

$$= \varepsilon_\infty + \sum_{i=1}^{n} \frac{\Delta\varepsilon_i}{1+(i\omega\tau_i)^{\alpha_i}} + j\frac{\sigma_{DC}}{\omega\varepsilon_0},$$

where CC_i is the relaxation process contribution described by the empirical Cole–Cole formula; ε_∞ is the phonon modes and electric polarizability contribution; $\Delta\varepsilon = \varepsilon - \varepsilon_\infty$; τ, s, is the most probable time (relaxation frequency ω), $\tau = 2\pi/\omega$; σ_{DC}, S/m, is the DC conductivity; α is the relaxation time distribution ($0 < \alpha < 1$).

The best way of approximating the frequency dependences was finding the sum of the contributions made by three relaxation processes; the processes differ in the most probable relaxation frequencies: one of the processes was observed in the frequency range of $f = 0.1–1$ Hz and had a monotone temperature dependence of the Δε

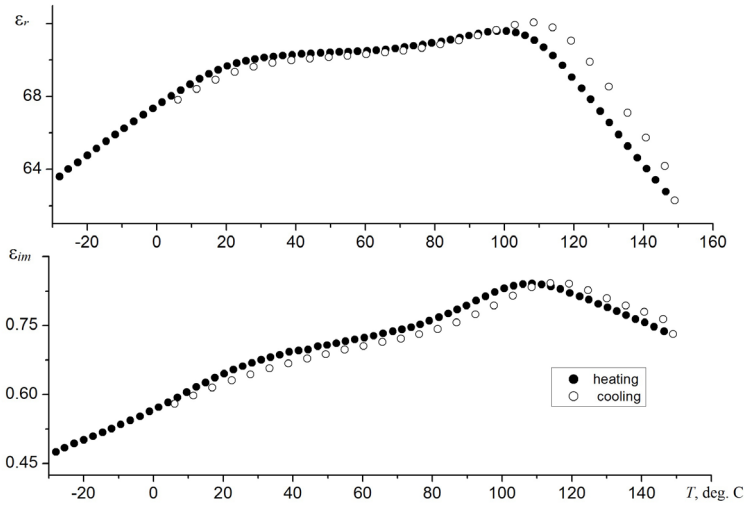

Fig. 2. Heating/cooling permittivity temperature dependences of the solid $BaZr_{0.1}Ti_{0.9}O_3$ solution; test frequency $f = 1.4$ kHz

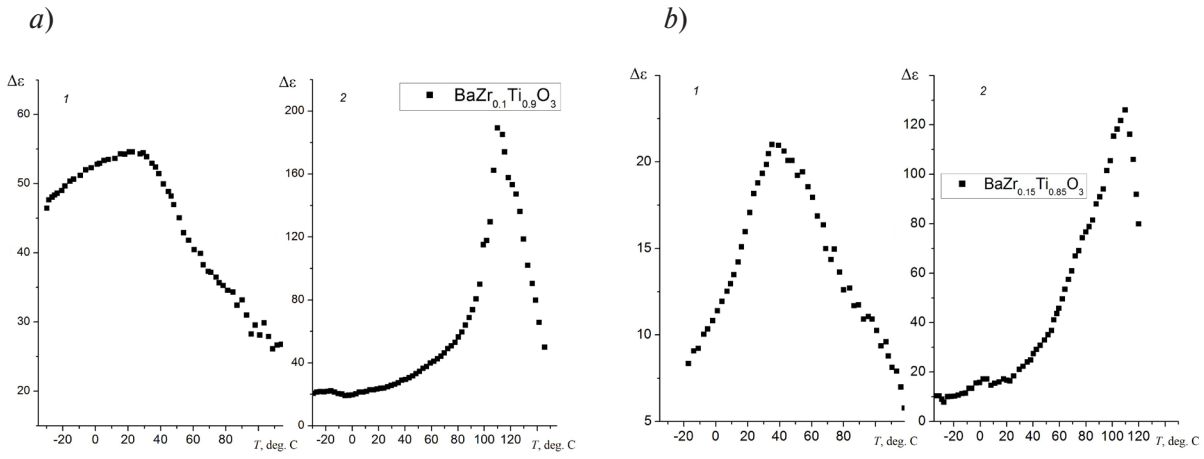

Fig. 3. Temperature dependences of the Δε parameter for relaxation processes *1* and *2* (see text) in solid solutions $BaZr_{0.1}Ti_{0.9}O_3$ (*a*) and $BaZr_{0.15}Ti_{0.85}O_3$ (*b*)

Table 2

Temperature values corresponding to peaks on Δε(*T*) dependences for relaxation processes *1* and *2* in the studied $BaTi_{1-x}Zr_xO_3$ samples

x value	Peak temperature, °C	
	Process *1*	Process *2*
0.01	31.6	118.5
0.03	36.9	115.6
0.10	27.4	112.4
0.15	35.9	111.2
0.20	42.1	109.6
0.30	27.8	113.9

N o t e. The presented results are obtained on the basis of dielectric measurements data. Processes *1* and *2* differ in the temperature ranges where their peaks were observed.

parameter; two other processes with different relaxation frequencies lying in the range of $f = 10^3 - 10^4$ Hz had peaks on the Δε(*T*) dependences at the temperature of around 27°C (process *1*) and around 109°C (process *2*) (Fig. 3). As an example, Fig. 3 presents the corresponding data for two studied samples.

Thus, we were able to identify the relaxation processes responsible for the phase transitions in the material under study. We used temperature dependences of the Δε parameter to determine the phase transition temperatures for each compound (Table 2). The peak temperatures Δε(*T*) for process *2* in all the samples was close to the temperature of the ferroelectric transition from the cubic into tetragonal phase in pure $BaTiO_3$ ($T_C = 120$°C) and solid solutions of $BaTi_{1-x}Zr_xO_3$ with low zirconium concentration. A small decrease in the temperature of this transition agrees with the phase diagram of the solid $BaTi_{1-x}Zr_xO_3$ solutions, according to which at low zirconium content the temperature of this transition decreases in these solutions [11].

The peaks of Δε(*T*) for relaxation process 1 in the samples of $BaTi_{1-x}Zr_xO_3$ are observed at temperatures close to the respective value of the transition between two ferroelectric phases of pure $BaTiO_3$ ($T = 5$°C) with the orthorhombic and tetragonal crystalline structures. The observed increase in the temperature of this transition agrees with the phase diagram of the solid $BaTi_{1-x}Zr_xO_3$

solutions in the range of small zirconium concentrations.

However, we should note that the temperature values of both phase transitions in all six samples vary insignificantly with the change of the assumed zirconium concentration in solutions and show no dependence on x [12]. This is probably due to the fact the main contribution to the dielectric response of the obtained solutions is made by the phase of the solid $BaTi_{1-x}Zr_xO_3$ solutions with low and approximately identical zirconium concentration of $x < 0.1$ for all the samples.

Diffuse reflectance spectra and integral absorption coefficient. A study of the diffuse reflectance spectra in the solar range of the synthesized powders necessary for finding the optimal concentration of the zirconium cations to obtain the $BaTi_{1-x}Zr_xO_3$ powder with high reflectance and low absorption coefficient as is of particular interest.

The diffuse reflectance spectra of the $BaTi_{1-x}Zr_xO_3$ powders were registered in the UV, visible and near infrared ranges. Fig. 4 presents the diffuse reflectance spectra of the synthesized powders with the concentration of substituting zirconium cations in the range from 0 to 30%.

For all concentrations of substituting zirconium cations, the reflectance coefficient of the $BaTi_{1-x}Zr_xO_3$ powders varies in the range of 85–96% in the area from the main absorption edge to 2200 nm. Qualitatively, the form of ρ spectra is practically identical for all the powders under study, at 1400 and 2040 nm wavelengths, there are absorption bands visible due to OH-groups located at the surface of the powder grains and granules of $BaTi_{1-x}Zr_xO_3$ [13]. In the area of the main absorption edge, as the zirconium concentration grows, we can observe a minor deterioration in reflectance.

It follows from the diffuse reflectance spectra shown in Fig. 4 that $BaTi_{1-x}Zr_xO_3$ powder has the highest reflectance in the visible and near infrared ranges at the zirconium concentration of $x = 0.05$, and the lowest reflectance at the concentration of $x = 0.15$. The difference in the reflection coefficient for different zirconium concentrations in one wavelength reaches 10%.

The integral absorption coefficient of solar radiation as was calculated based on the diffuse reflection coefficient using the following formula:

$$a_s = 1 - R_s = 1 - \frac{\int_{\lambda_1}^{\lambda_2} \rho_\lambda I_\lambda d\lambda}{\int_{\lambda_1}^{\lambda_2} I_\lambda d\lambda} = 1 - \frac{\sum_{i=1}^{n} \rho_\lambda}{n},$$

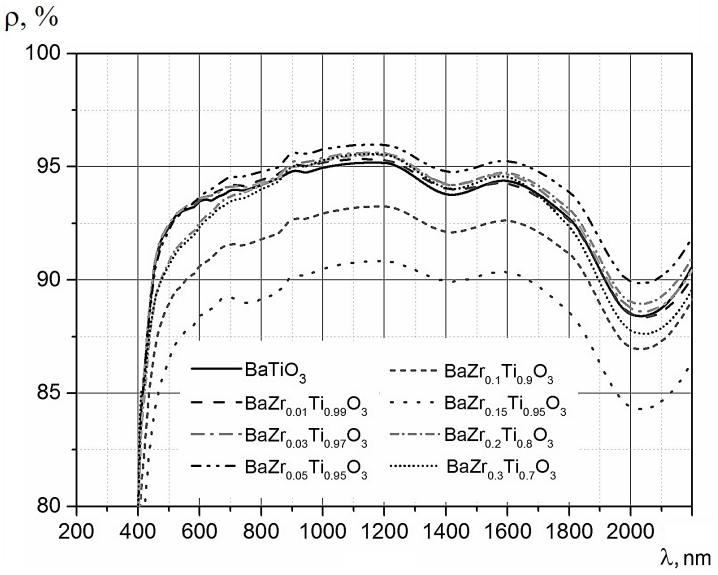

Fig. 4. Diffuse reflectance spectra of solid $BaTi_{1-x}Zr_xO_3$ solutions with different content of substituting zirconium cations

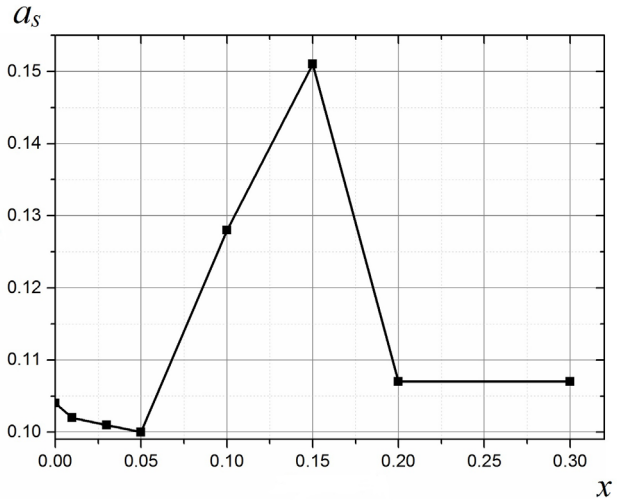

Fig. 5. Dependence of the integral absorption coefficient of solar radiation on zirconium content in the solid $BaTi_{1-x}Zr_xO_3$ solution

Table 3

Values of the integral absorption coefficient of solar radiation for the $BaTi_{1-x}Zr_xO_3$ powders at different values of x

x	0.00	0.01	0.03	0.05	0.10	0.15	0.20	0.30
a_s	0.104	0.102	0.101	0.100	0.128	0.151	0.107	0.107

N o t e. The presented results are obtained by means of calculations on the basis of the diffuse solar radiation reflectance spectra.

where R_s is the integral absorption coefficient of solar radiation calculated as the arithmetic mean value of the reflection coefficient over 24 points located in equal-energy areas of the solar radiation spectrum according to the international standards [14, 15]; ρ_λ is the spectral reflectivity; I_λ is the solar radiation spectrum; λ_1, λ_2, μm, are the boundary values of the solar spectrum range (in the area of 0.2–2,5 μm the sun radiates 98% of the total energy); n is the number of equal-energy areas of the solar spectrum given by the standard tables [14, 15].

As you can see from Table 3, all synthesized powders have rather low integral absorption coefficients of solar radiation in the range from 0.100 to 0.151 and can fall into the class of "solar reflectors". The $BaTi_{1-x}Zr_xO_3$ powder with 5% of zirconium cations ($x = 0.05$) possesses the smallest value of a_s (0.100), while the powder with 15% of zirconium ($x = 0.15$) has the greatest value.

Fig. 5 presents a dependence of a_s on the percentage of the substituting zirconium cations in the range from 0 to 30% (x = 0–0.30). As the zirconium cations concentration in the $BaTi_{1-x}Zr_xO_3$ compounds increases, the integral absorption coefficient of solar radiation changes based on a rather complex dependence with a minimum and a maximum. The highest values of as are observed at 10 and 15 % zirconium concentrations.

Conclusion

We used the solid-phase synthesis method with a two-step heating to produce $BaTi_{1-x}Zr_xO_3$ powders from a mixture of micron-sized $BaCO_3$, ZrO_2 and TiO_2 powders at concentration of substituting zirconium cations in the range of 0–30 weight % (x = 0.01–0.30). We studied the dependences of the particle-size distribution, phase composition, diffuse reflectance spectra in the

UV, visible and near infrared ranges, and the integral absorption coefficient of solar radiation as on the zirconium cations concentration. The established maximum yield of the main powder phase amounts to 90.3%. The form of the diffuse reflectance of the synthesized $BaTi_{1-x}Zr_xO_3$ micro powders varies insignificantly depending on the zirconium concentration; however, the qualitative changes reach 10%. The integral absorption coefficient of the studied powders at different zirconium concentration varied within 34%. The conducted dielectric research of the pressed powders revealed two peaks on the permittivity temperature dependences associated with the phase transitions. We determined the temperatures of these phase transitions for all compositions and revealed that the low temperature transition in the solutions under study was observed at room temperatures. This fact makes these compounds a promising material for production of pigments for thermal control coatings at operating temperatures of space crafts.

The study was financially supported by the Russian Foundation for Basic Research as part of scientific project no. 19-32-60067.

REFERENCES

1. **Li Q., Fan D., Xuan Y.,** Thermal radiative properties of plasma sprayed thermochromic coating, Journal of Alloys and Compounds. 583 (25 February) (2014) 516–522.

2. **Green N.W., Kim W., Low N., et al.,** Electrostatic discharges from conductive thermal coatings, IEEE Transactions on Plasma Science. 47 (8-2) (2019) 3759–3765.

3. **Yamamoto T., Sato Y., Tanaka T., et al.,** Electron transport behaviors across single grain boundaries in *n*-type $BaTiO_3$, $SrTiO_3$ and ZnO, Journal of Materials Science. 40 (4) (2005) 881– 887.

4. **Lee J.H., Nersisyan H.H., Lee H.H., Won C.W.,** Structural change of hydrothermal $BaTiO_3$ powder, Journal of Materials Science. 39 (4) (2004) 1397–1401.

5. **Rout S.K.,** Phase formation and dielectric studies of some $BaO\text{-}TiO_2\text{-}ZrO_2$ based perovskite system, A thesis in physics (Materials Science), April 2006, Department of Physics, National Institute of Technology, Rourkela-769 008 (A Deemed University) Orissa, India, 2006.

6. **Wang H., Cao X., Liu F., et al.,** Synthesis and electrochemical properties of transparent nanostructured $BaTiO_3$ film electrodes, Open Journal of Inorganic Chemistry. 5 (2) (2015) 30–39.

7. **Mikhailov M.M., Ul'yanitskii V.Yu., Vlasov V.A., et al.,** Thermostabilizing $BaTiO_3$ coatings synthesized by detonation spraying method, Surface Coating Technology. 319 (15 June) (2017) 70–75.

8. **Ho C., Fu S.-L.,** Effects of zirconium on the structural and dielectric properties of (Ba, Sr) TiO_3 solid solution, Journal of Materials Science. 25 (11) (1990) 4699–4703.

9. **Son S.Y., Kim B.S., Oh S.H., et al.,** Electrical properties of (Ba, Sr) TiO_3 on (Sr, Ca) RuO_3 electrode, Journal of Materials Science. 34 (24) (1999) 6115–6119.

10. **Saburi O., Wakino K., Fuzikawa N.,** Semiconductors based on barium titanate, Tokyo, 1977.

11. **Gorev M., Bondarev V., Flerov I., et al.,** Heat capacity study of double perovskite-like compounds $BaTi_{1-x}Zr_xO_3$, Physics of the Solid State. 47 (12) (2005) 2304–2308.

12. **Shvartsman V.V., Zhai J., Kleemann W.,** The dielectric relaxation in solid solutions $BaTi_{1-x}Zr_xO_3$, Ferroelectrics. 379 (1) (2009) 77–85.

13. **Cronemeyer D.C.,** Infrared absorption of reduced rutile TiO_2 single crystals, Physical Review. 113 (5) (1959) 1222–1226.

14. ASTM E490 – 00a Standard Solar Constant and Zero Air Mass Solar Spectral Irradiance Tables. 2005. https://www.astm.org/Standards/E490.htm

15. ASTM E903 – 96 Standard Test Method for Solar Absorptance, Reflectance, and Transmittance of Materials Using Integrating Spheres. 2005. https://www.astm.org/DATABASE.CART/HISTORICAL/E903-96.htm

Received 31.03.2021, accepted 27.04.2021.

THE AUTHORS

MIKHAILOV Mikhail M.
Tomsk State University of Control Systems and Radioelectronics
40, Lenin Ave. Tomsk, 634050, Russian Federation
membrana2010@mail.ru

ALEKSEEVA Olga A.
Tomsk State University of Control Systems and Radioelectronics
40, Lenin Ave. Tomsk, 634050, Russian Federation
blackhole2010@yandex.ru

YURYEV Semen A.
Tomsk State University of Control Systems and Radioelectronics
40, Lenin Ave. Tomsk, 634050, Russian Federation
semyon.yuryev@tusur.ru

LAPIN Alexey N.
Tomsk State University of Control Systems and Radioelectronics
40, Lenin Ave. Tomsk, 634050, Russian Federation
alexey.lapin@tusur.ru

KOROLEVA Ekaterina Yu.
Peter the Great St. Petersburg Polytechnic University
29 Politechnicheskaya St., St. Petersburg, 195251, Russian Federation
e.yu.koroleva@mail.ioffe.ru

СПИСОК ЛИТЕРАТУРЫ

1. **Li Q., Fan D., Xuan Y.** Thermal radiative properties of plasma sprayed thermochromic coating // Journal of Alloys and Compounds. 2014. Vol. 583. 25 February. Pp. 516–522.

2. **Green N.W., Kim W., Low N., Zhou Ch., Andersen A., Linton T., Martin E.** Electrostatic discharges from conductive thermal coatings // IEEE Transactions on Plasma Science. 2019. Vol. 47. No. 8. Part 2. Pp. 3759–3765.

3. **Yamamoto T., Sato Y., Tanaka T., Hayashi K., Ikuhara Y., Sakuma T.** Electron transport behaviors across single grain boundaries in *n*-type $BaTiO_3$, $SrTiO_3$ and ZnO // Journal of Materials Science. 2005. Vol. 40. No. 4. Pp. 881–887.

4. **Lee J.H., Nersisyan H.H., Lee H.H., Won C.W.** Structural change of hydrothermal $BaTiO_3$ powder // Journal of Materials Science. 2004. Vol. 39. No. 4. Pp. 1397–1401.

5. **Rout S.K.** Phase formation and dielectric studies of some $BaO\text{-}TiO_2\text{-}ZrO_2$ based perovskite system. A thesis in physics (Materials Science). April 2006. Department of Physics. National Institute of Technology. Rourkela-769 008 (A Deemed University) Orissa, India. 166 p.

6. **Wang H., Cao X., Liu F., Guo S., Ren X., Yang S.** Synthesis and electrochemical properties of transparent nanostructured $BaTiO_3$ film electrodes // Open Journal of Inorganic Chemistry. 2015. Vol. 5. No. 2. Pp. 30–39.

7. **Mikhailov M.M., Ul'yanitskii V.Yu., Vlasov V.A., Sokolovskiy A.N., Lovitskii A.A.** Thermostabilizing $BaTiO_3$ coatings synthesized by detonation spraying method // Surface and Coating Technology. 2017. Vol. 319. 15 June. Pp. 70–75.

8. **Ho C., Fu S.-L.** Effects of zirconium on the structural and dielectric properties of (Ba, Sr) TiO_3

solid solution // Journal of Materials Science. 1990. Vol. 25. No. 11. Pp. 4699–4703.

9. **Son S.Y., Kim B.S., Oh S.H., Choi D.K., Yoo C.C., Lee S.I., Dai Z.R., Ohuchi F.S.** Electrical properties of (Ba, Sr)TiO_3 on (Sr, Ca)RuO_3 electrode // Journal of Materials Science. 1999. Vol. 34. No. 24. Pp. 6115–6119.

10. **Сабури О., Вакино К., Фудзикава Н.** Полупроводники на основе титаната бария. Пер. с японского яз. М.: Энергоиздат, 1982. 53 с.

11. **Горев М.В., Бондарев В.С., Флёров И.Н., Сью Ф., Саварио Ж.-М.** Исследования теплоемкости двойных перовскитоподобных соединений $BaTi_{1-x}Zr_xO_3$ // Физика твердого тела. 2005. Т. 47. № 12. С. 2212–2216.

12. **Shvartsman V.V., Zhai J., Kleemann W.** The dielectric relaxation in solid solutions $BaTi_{1-x}Zr_xO_3$ // Ferroelectrics. 2009. Vol. 379. No. 1. Pp. 77–85.

13. **Cronemeyer D.C.** Infrared absorption of reduced rutile TiO_2 single crystals // Physical Review. 1959. Vol. 113. No. 5. Pp. 1222–1226.

14. ASTM E490 – 00a standard solar constant and zero air mass solar spectral irradiance tables. 2005. https://www.astm.org/Standards/E490.htm

15. ASTM E903 – 96 standard test method for solar absorptance. Reflectance, and transmittance of materials using integrating spheres. 2005. https://www.astm.org/DATABASE.CART/HISTORICAL/E903-96.htm

Статья поступила в редакцию 31.03.2021, принята к публикации 27.04.2021.

СВЕДЕНИЯ ОБ АВТОРАХ

МИХАЙЛОВ Михаил Михайлович – *доктор физико-математических наук, профессор, заведующий лабораторией радиационного и космического материаловедения Томского государственного университета систем управления и радиоэлектроники, г. Томск, Российская Федерация.*

634050, Российская Федерация, г. Томск, пр. Ленина, 40

membrana2010@mail.ru

АЛЕКСЕЕВА Ольга Александровна – *кандидат физико-математических наук, старший научный сотрудник лаборатории радиационного и космического материаловедения Томского государственного университета систем управления и радиоэлектроники, г. Томск, Российская Федерация.*

634050, Российская Федерация, г. Томск, пр. Ленина, 40

kblackhole2010@yandex.ru

ЮРЬЕВ Семен Александрович – *кандидат технических наук, старший научный сотрудник лаборатории радиационного и космического материаловедения Томского государственного университета систем управления и радиоэлектроники, г. Томск, Российская Федерация.*

634050, Российская Федерация, г. Томск, пр. Ленина, 40

semyon.yuryev@tusur.ru

ЛАПИН Алексей Николаевич – *кандидат технических наук, старший научный сотрудник лаборатории радиационного и космического материаловедения Томского государственного университета систем управления и радиоэлектроники, г. Томск, Российская Федерация.*

634050, Российская Федерация, г. Томск, пр. Ленина, 40

alexey.lapin@tusur.ru

КОРОЛЕВА Екатерина Юрьевна – *кандидат физико-математических наук, старший научный сотрудник научно-образовательного центра «Физика нанокомпозитных материалов электронной техники» Санкт-Петербургского политехнического университета Петра Великого, Санкт-Петербург, Российская Федерация.*

195251, Российская Федерация, г. Санкт-Петербург, Политехническая ул., 29

e.yu.koroleva@mail.ioffe.ru